

Article ID: 1006-8775(2015) 01-0076-08

VARIATION OF AEROSOL OPTICAL CHARACTERISTICS IN GUANGZHOU DURING SOUTH CHINA SEA SUMMER MONSOON EVENTS

ZHENG Bin (郑彬), WU Dui (吴兑), LI Fei (李菲), DENG Tao (邓涛)

(Guangzhou Institute of Tropical and Marine Meteorology/Key Laboratory of Regional Numerical Weather Prediction, China Meteorological Administration, Guangzhou 510080 China)

Abstract: Variations in Guangzhou's aerosol optical characteristics and their possible causes are studied against the large-scale background of South China Sea summer monsoons (SCSSM) using aerosol data derived from Panyu Atmospheric Composition Watch Station in Guangzhou and the National Centers for Environmental Prediction/National Center for Atmospheric Research (USA). The data is reanalyzed to develop a composite analysis and perform physical diagnoses. Analysis of the results shows that aerosol extinction in Guangzhou first increases then decreases during the active period of a SCSSM, with variations in the stratification of the planetary boundary layer (PBL) and environmental winds playing important roles in affecting Guangzhou's aerosol optical characteristics. Regional diabatic heating and anomalous cyclonic circulations excited by monsoon convection induce environmental wind anomalies that significantly modify the stratification of the PBL.

Key words: aerosol optical characteristics; composite analysis; South China Sea summer monsoon

CLC number: P462.41 **Document code:** A

1 INTRODUCTION

The term "atmospheric aerosol" generally refers to solid or liquid particles suspended in the atmosphere, which can come from natural processes or human activities and range from nanometers to tens of microns in diameter. Natural particle sources include volcanic ash, cosmic dust, pollen, seawater droplets, soil dust, and so on. Since the age of industrialization, human activities have directly discharged a large number of particles and pollution gas into the atmosphere, the latter also transforming into aerosol particles such as sulfate, nitrate, ammonium salt, organic carbon, elemental carbon, and mineral elements through heterogeneous chemical reactions. Aerosol research began in the middle of the 19th century with Tyndall's aerosol optical experiment in 1869 and Rayleigh's light scattering theory in 1871. As aerosols have a significant influence on climate change, cloud physics, visibility, environmental quality, cycling of atmospheric trace elements, and human health, research in the field developed rapidly through the 20th century, gradually becoming a multi-interdisciplinary research field in the 1970s. More recently, scientists not

only revealed a correlation between atmospheric aerosols and climate change (Babu and Moorthy^[1]; Meinrat^[2]; Menon et al.^[3]; Houghton et al.^[4]), but also proved atmospheric aerosols' radiation effect on climate change through numerous experiments (Ramanathan et al.^[5]; Won et al.^[6]; Lau et al.^[7]), observation and data analysis (Jacobson^[8]; Lohmann and Lesins^[9]; Cao et al.^[10]; Penner et al.^[11]), and numerical simulation (Su et al.^[12]; Deng et al.^[13]). As an essential constituent for global change, the effects of aerosol radiation has become an important topic of wide concern by scientists and one of the hot issues of current global change research (Reddy and Venkataraman^[14]; Wang et al.^[15]; Chen et al.^[16]).

Monsoon-induced floods, droughts, and other natural disasters threaten more than 60% of the global population. As a result, the effects of aerosol radiative forcing on large-scale monsoon systems have received considerable attention in the last 10 years. Previous studies have shown that aerosol radiative forcing can affect the rainfall or rainband distribution in the South Asian monsoon (Zhou et al.^[17]; Devara et al.^[18]; Chen et al.^[19]), the East Asian monsoon (Gu et al.^[20]; Huang et al.^[21]), the African monsoon (Siknib et al.^[22]; Huang et al.^[23]), and the South American monsoon (Lin et al.^[24]). While there has been a considerable amount of research studying this relationship between aerosol radiative forcing and monsoons, there is still a lack of observational data. Many of these studies use model aerosol distributions to simulate radiative forcing, which leads to more uncertainty in the analysis. On the other hand, different aerosol distributions can cause a significant difference in radiative effects due to large spatial and temporal variations. Therefore, it is very important to fully define the spatial and temporal variations of an

Received 2013-08-27; **Revised** 2014-12-15; **Accepted** 2015-01-15

Foundation item: Major State Basic Research Development Program (973 Program) of China (2011CB403403; Guangdong Science and Technology Planning Project (2012A061400012, 2012A030200006); National Natural Science Foundation of China (41205069)

Biography: ZHENG Bin, Ph. D., associate professor, primarily undertaking research on monsoon and air-sea interactions and middle atmosphere.

Corresponding author: ZHENG Bin, e-mail: zbin@grmc.gov.cn

aerosol based on observational data.

In recent years, aerosol pollution over the Pearl River Delta region has become increasingly serious, leading to a worsening in visibility. Analysis of the aerosol optical thickness distribution from EOS/MODIS satellite remote sensing data indicates that atmospheric aerosol pollution over the Pearl River Delta urban areas is getting more serious than the aerosol pollution over surrounding areas (Wu^[25]). Therefore, to study the climatic effects of aerosols in the Pearl River Delta, we must understand the spatial and temporal distribution characteristics of the aerosols and the reasons for these differences. Previous research in the topic has often used local weather conditions to explain this distribution of aerosols. From a climatology viewpoint, however, we also do not know much about the variations occurring within the large-scale climatic background of the area. Thus, this paper uses the aerosol data collected at Panyu Atmospheric Composition Watch Station (AC-Watch) in Guangzhou to study the variation and its possible causes in Guangzhou's aerosol optical characteristics over the large-scale regions affected by South China Sea summer monsoons (SCSSM).

2 DATASETS

In this paper, the daily aerosol absorption coefficient (532 nm) and scattering coefficient (525 nm) were calculated from instrument observations at AC-Watch in Guangzhou. The absorption coefficient was derived by substituting the black carbon density measured into Eq. (3) of Wu et al.^[26] using an aethalometer (Magee scientific, AE31), while the scattering coefficient was measured by a turbidimeter (Ecotech, M9003). Variables describing the monsoon background—consisting of u and v winds, air temperature, specific humidity, net longwave and shortwave radiations, and sensible heat flux—came from the National Centers for Environmental Prediction (NCEP)/National Center for Atmospheric Research (NCAR) reanalysis data (Kalnay et al.^[27]). Moreover, GPCP Satellite-Derived (IR) GPI Daily Rainfall (Janowiak and Arkin^[28]) is also used in the paper. All of the data span from May to September in 2008 and 2009. A 5-d running mean has been made in all the data to remove, to some extent, high-frequency signals. According to Zheng et al.^[29], we define a circulation index (CI) using Eqs. (1) and (2) to describe monsoon activity

$$I_u = u_{200} - u_{850}, (105^\circ \text{ to } 120^\circ \text{ E mean}) \quad (1)$$

$$I_v = v_{200} - v_{850}, (105^\circ \text{ to } 120^\circ \text{ E mean}) \quad (2)$$

The circulation conditions of SCSSM activity are reached when both I_u and I_v are less than zero and there are opposite signs for winds in the upper and lower troposphere, respectively. We define a period of SCSSM activity as having a positive precipitation departure averaged over the region bounded by 105° - 120° E and 5° - 20° N, maintained over one or more pentad (5 days). Note that the SCSSM activity can be described more

accurately by defining the SCSSM activity using both circulation and convection (Zheng and Meng^[30]). In addition, an obvious CI center near 5° N during the period of SCSSM activity indicates significant activity. The South China Sea (SCS) region in this paper is the region 105° - 120° E, 5° - 20° N, where SCSSMs are active and the activity conditions are met in all other regions which are affected by the SCSSM.

3 DATA ANALYSIS

3.1 SCSSM activity and aerosol optical characteristics in Guangzhou

Figure 1a shows the average change in precipitation in the SCS region over time through the observed period of 2008. Note that there are 5 periods of continuous positive departures corresponding to areas of a CI less than zero (Fig. 1b). Within these 5 periods, significant SCSSM activities occur in the three periods of 9 to 17 May, 22 July to 11 August, and 6 to 30 September, as defined by their high center of CI values near 5° N. The maximum CI values for these periods occur on 15 May, 3 August, and 25 September, respectively. These data indicate that the SCSSM was very active during these three periods. On the other hand, there are no evident CI centers for the two periods of 20 to 24 June and 2 to 8 July, even though the precipitation changes are positive, thus indicating that the SCSSM activity in these periods was relatively weaker. Fig. 1c shows the standardization of the Guangzhou aerosol absorption coefficient (solid line) and the scattering coefficient (dotted line). Standardization is defined as the original value divided by its standard deviation, which provides a unit less standardized value with a variance of 1. We can see from Fig. 1c that the optical characteristics of

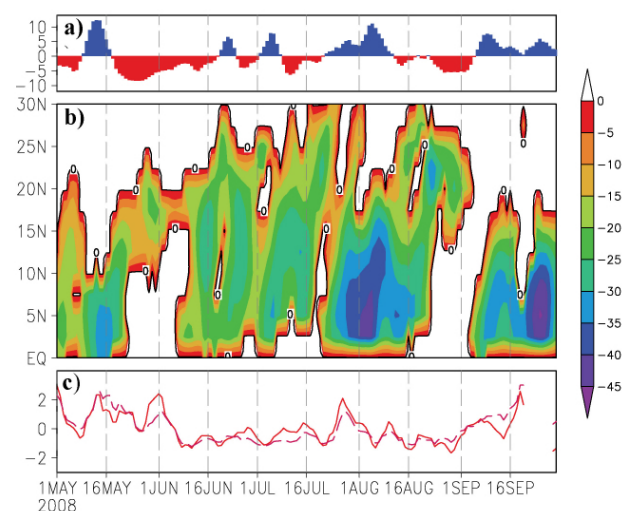


Figure 1. (a) Precipitation changes (mm) averaged in the South China Sea region (105° to 120° E, 5° to 20° N); (b) South China Sea summer monsoon circulation index (m/s), where shaded areas denote both meridional and zonal circulation indices that are less than zero; and (c) standardized aerosol absorption (solid line) and scattering (dash line) coefficients. All data is over the period from May to September 2008.

Guangzhou aerosols possess significant intraseasonal variations, especially during SCSSM's active period. Following the start of each typical SCSSM activity, Guangzhou aerosol extinction properties increase and reach the maximum on the most active day of the SCSSM before weakening again.

Figure 2 shows the 4 active periods of the SCSSM in 2009, corresponding to 9 to 21 July, 28 July to 4 August, 30 August to 14 September, and 20 to 30 September, respectively. Corresponding CI centers occur on 15 July, 3 August, 8 September, and 25 September, respectively. Fig. 2c shows that the Guangzhou aerosol extinction between May and September of 2009 first increases then decreases during each active SCSSM period. In order to highlight this change, we made a composite analysis using the reference date according to the active CI center. Although aerosol extinction has an interannual variation, this extinction has little effect on intraseasonal time scales because the aerosol extinction is a change relative to the mean of each SCSSM period. Since there is a lack of aerosol extinction characteristics in late September 2008, the composite analysis excludes the period of 6 to 30 September. Both Fig. 1 and Fig. 2 show that the CI center occurs in the mid- and late-period of each active SCSSM, so each composite consists of data from 10 days before the reference day to 5 days after it (Fig. 3).

We can see from Fig. 3a and 3b, which shows the active SCSSM period from -7 days to +5 days, that there is a period of high precipitation over the SCS region when the CI reaches its extreme, then decreases as the absolute value of the CI decreases. Fig. 3c and 3d illustrates that both the composite Guangzhou aerosol absorption coefficient and the scattering coefficient weaken after an initial increase. However, the absorption coefficient reaches the maximum a few days before the reference date, while the maximum scattering coefficient appears several days after the reference date.

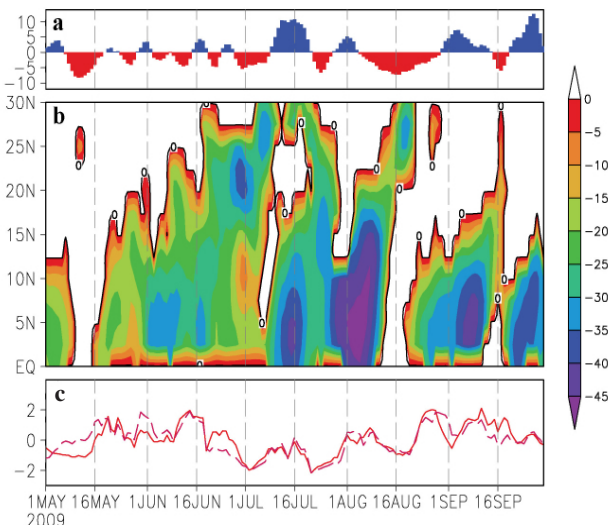


Figure 2. Same as Fig.1 but for the period encompassing May to September 2009.

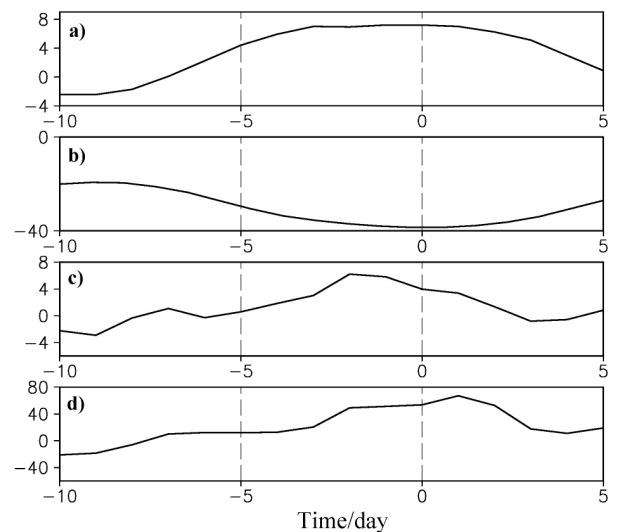


Figure 3. (a) composites of the precipitation changes averaged in the SCS region (mm); (b) 105° to 120°E, 5° to 7.5°N averaged SCSSM circulation index (m/s); (c) Guangzhou aerosol absorption coefficient departure (mm^{-1}); and (d) scattering coefficient departure (mm^{-1}). Time zero denotes the reference date corresponding to the circulation index center, where a negative time represents the days before the reference date and a positive time the days after.

3.2 SCSSM effects on the optical characteristics of Guangzhou aerosols

3.2.1 STRATIFICATION VARIATIONS OF THE PLANETARY BOUNDARY LAYER

Aerosol extinction coefficients are prone to increase over time when subjected to bad diffusion due to stable stratification of the planetary boundary layer (PBL). Fig. 4 shows the rate of change in temperature (averaged over the 115°-120° E, 22.5°-25° N region). When the SCSSM is active, PBL stratification tends to stabilize. The stratification starts to become unstable 3 days prior to the reference date, a result consistent with an evident curve in temporal variations of the extinction coefficients (see Fig. 3c and 3d) even though the scattering coefficient increases until to 2 days after the reference date. This result reveals the evident effects of stratification variation on aerosol absorption and scattering coefficients, as well as the latter being affected by other important factors in the early active stages of the SCSSM. Moreover, Fig. 4 shows that stratification of the PBL becomes more and more stable up to the day when the SCSSM is most active. However, the absorption coefficient still decreases during this same period, while the scattering coefficient also begins to decrease 1 day after the reference date. This implies that there are other more important factors than the stratification of temperature impacting the extinction coefficient in the late active stage of SCSSM.

The following analysis focuses on understanding the reason why extremum appear on the relative days -5 and -1; the extremum on date +2 is neglected since the

stratification is not a key factor of the extinction coefficient at this stage. The variation in the temperature over

time is mainly due to advection, adiabatic, and diabatic heating (see Fig. 5).

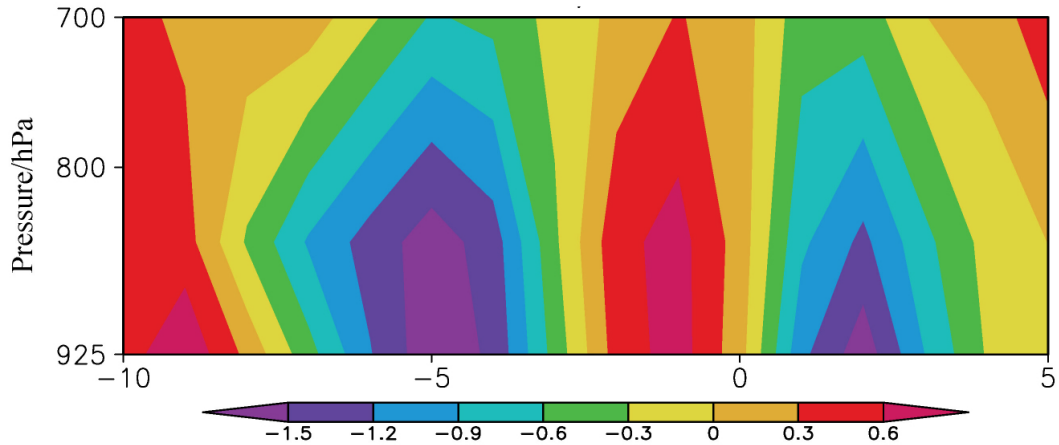


Figure 4. Composite of the rate of change in temperature ($10^{-6} \times \text{K/s}$) averaged over 15° to 120°E , 22.5° to 25°N . Time zero denotes the reference date corresponding to the circulation index center, where a negative time represents the days before the reference date and a positive time indicates the days following it.

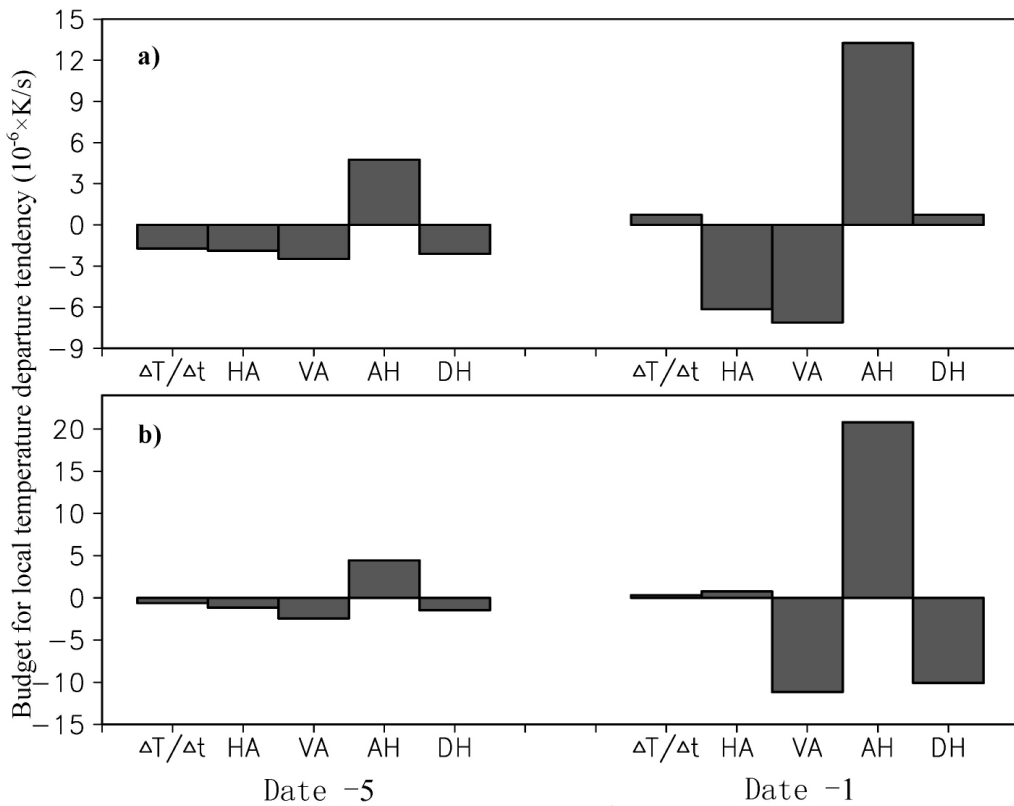


Figure 5. Composite analysis of the rate of change in local temperature ($10^{-6} \times \text{K/s}$), averaged over the region of 115° to 120°E : (a) 925 hPa and (b) 700 hPa. The left image is for the day -5, while the right image is for the day -1. Here, $\Delta T/\Delta t$ is the local change in temperature over time, HA is the horizontal advection, VA is the vertical advection, AH is the adiabatic heat flux, and DH is the diabatic heat flux.

The horizontal advection can be written as

$$\text{HA} = -u\left(\frac{\partial T}{\partial x} - v\frac{\partial T}{\partial y} + u\frac{\partial \bar{T}}{\partial x} + v\frac{\partial \bar{T}}{\partial y}\right) \quad (3)$$

where “ $\bar{\quad}$ ” denotes the time average. In this paper, time

is averaged from 1 May to 30 September in 2008 and 2009. The vertical advection is

$$\text{VA} = -\omega \frac{\partial T}{\partial p} \quad (4)$$

while the adiabatic heat flux is written as

$$AH = -\omega \frac{RT}{c_p P} \quad (5)$$

and the diabatic heat flux as

$$DH = \Delta T / \Delta t - HA - VA - AH \quad (6)$$

The left panel of Fig. 5a illustrates the rate of change in temperature over the time averaged over 115°-120°E, 22.5°-25°N at 925 hPa on day -5. The signs for the advection and diabatic terms of the local temperature change express the positive impact with the larger contribution coming from the vertical advection term. The right image of Fig. 5a shows that both the adiabatic and diabatic heat have the same sign as the shift in local temperature on day -1 at 925 hPa, and the adiabatic heat term almost balances that for advection. Fig. 5b displays very little local temperature change at 700 hPa five days and one day before the CI maximum (-5 and -1), but significant amount of advection, adiabatic, and diabatic heat flux. In addition, Fig. 5 indicates that the vertical advection term is always negative while the adiabatic heat flux is always positive. Note that, on these two days, the pressure vertical velocity in the PBL is positive, resulting in sinking motion and adiabatic heating. Meanwhile, the vertical mean temperature gradients are downwards while anomalous temperatures are climbing, leading to little negative vertical advection.

Our calculations of the net surface longwave radiation, shortwave radiation, and sensible heat flux (figure omitted), indicate that the net heat flux cooled the surface air on day -5, a result consistent with the diabatic term in the left panel of Fig. 5a. On the other hand, the net heat flux on day -1 warmed the surface air, resulting in the positive diabatic term shown in the right image of Fig. 5a.

The above analysis shows that the rate of change in temperature is a key factor affecting variations in the stratification of the PBL. From the initial active phase to 1 day before the mature active phase, the advection contribution on temperature rate of change, averaged over the region of 115°-120°E, 22.5°-25°N, shifted from a positive effect to a negative one, while the adiabatic term shifted in the opposite way. Note that the diabatic term was positive throughout this entire period.

3.2.2 CHANGE OF HORIZONTAL WINDS

Winds are composed of mean winds and variations in those winds. Fig. 6 shows the mean winds at 925 hPa, which consists of a weak leaning south wind over the region of 115°-120°E, 22.5°-25°N and a strong southwesterly wind over the SCS during the SCSSM. Therefore, the winds of the 115°-120°E, 22.5°-25°N region are derived from the SCS southwesterly and the southeasterly of the western Pacific high. The evolution of the composite wind changes is shown in Fig. 7.

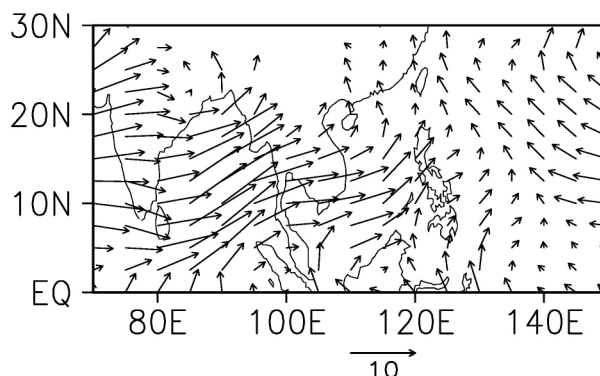


Figure 6. Winds (m/s) averaged over the period 1 May to 30 September in 2008 and 2009 at 925 hPa.

Fig. 7a indicates the presence of a non-active SCSSM in the 2 pentads (10 days) before the mature active phase. As a result, the cyclonic anomalous circulation does not appear over the SCS, but instead over the western North Pacific. There are also weak southerly anomalous winds over the region of 115°-120°E, 22.5°-25°N, which enhances the mean wind speed. The mean wind is 1.83 m/s, while the strengthened wind speed is 2.98 m/s. At this stage, both the anomalous winds and the stratification of the PBL (Fig. 4) benefit the aerosol diffusion, which consequently weakens the total aerosol extinction characteristics (Fig. 4c and 4d).

In the pentad before the mature active phase of the SCSSM, the monsoon becomes more and more active. At this point, the vortex center is east of the Philippines, with anomalous cyclonic vorticity occurring over the SCS (Fig. 7b). The northwest of the cyclonic circulation covers the region of 115°-120°E, 22.5°-25°N with an anomalous wind opposite of the mean wind direction, resulting in a generally decreased wind speed that decreases aerosol diffusion.

SCS convection is strongest in the active period of the mature phase of the SCSSM when the formed anomalous cyclonic vorticity is maximum (Fig. 7c). In this period, the region of 115°-120°E, 22.5°-25°N lies to the north of the circulation, where the anomalous wind vigorously competes against the mean wind, resulting in a wind speed of 4.66 m/s that favors increased aerosol diffusion. This explains why the aerosol absorption coefficient begins to decrease at this stage and why the scattering coefficient displays an evident step in the few days before the SCSSM active mature phase. This analysis also explains, at least in part, the question of why the aerosol extinction coefficient is still small at this stage, since the stratification of the PBL tends to stabilize after the active mature phase of the SCSSM.

In the first pentad after the active mature phase of the SCSSM, the monsoon marches northwards and affects the north region of the SCS. At this point, its convective center and cyclonic circulation shift northwards and the region of 115°-120°E, 22.5°-25°N is now situat-

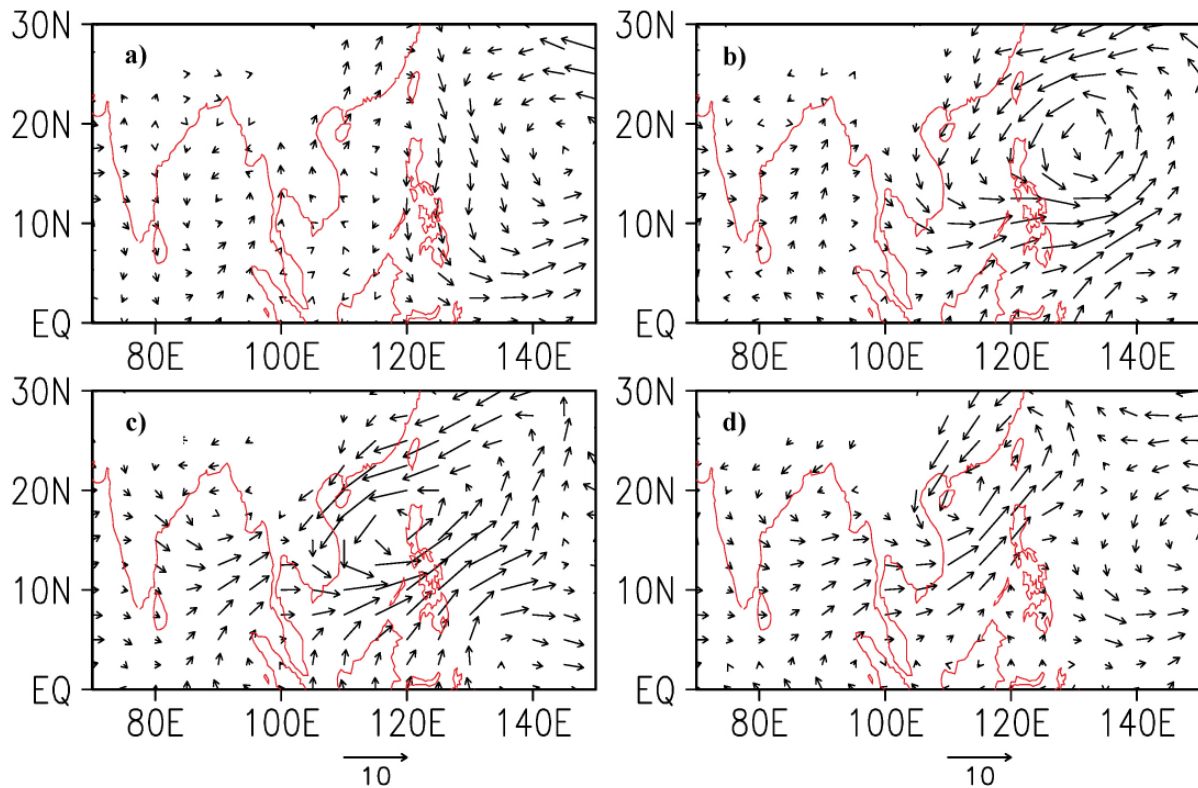


Figure 7. Composite changes in anomalous winds (m/s) at 925 hPa: (a) day -10, (b) day -5, (c) day 0, and (d) day +5.

ed at the edge of the circulation center. Although in some areas the anomalous wind is weak, the average regional wind is still relatively strong, continuously accelerating aerosol diffusion.

4 CONCLUSIONS AND DISCUSSIONS

(1) During the active period of the SCSSM, the Guangzhou aerosol extinction coefficient first increases and then decreases, with the transition date occurring during the active mature phase of the SCSSM. The absorption coefficient reaches its maximum value 2 days before the mature phase, while the scattering coefficient achieves its maximum value 1 day after the mature phase.

(2) In the active period of the SCSSM, diabatic processes play a continual important role in affecting PBL stratification. The advection term positively contributes to the change of PBL stratification in the early active stage of the SCSSM but restrains its change in the mature phase. The effect of the adiabatic term is contrary to the effect of the advection term.

(3) In the early active stage of a SCSSM, the anomalous and mean flows have opposite directions of approximately the same magnitude over the region of 115°-120°E, 22.5°-25°N, which decreases overall wind speed. In the mature and late stages, however, convection lies in the SCS and gradually moves northward. At this point, the anomalous flows in the northern circulation are significantly stronger than the mean flows,

which increases wind speed over the region.

(4) In the early and mature active stages of a SCSSM, the regional PBL stratification changes from a stable to an unstable state, while wind speed increases. These environmental conditions cause aerosol changes in the region to shift from accumulation to diffusion, while the extinction coefficient changes from an increasing value to a decreasing one. In the late active phase of the SCSSM, the regional PBL stratification tends to stabilize, but the strong wind speed continues to enhance aerosol diffusion. Therefore, the aerosol extinction coefficient continues to decrease, or at best remains static, during this late active phase.

Large regional wind speeds generally play a more important role than PBL stratification in affecting aerosol distribution. When the wind is not strong enough and as PBL stratification stabilizes, these two effects can balance one another. As shown in Fig. 3c and 3d, Fig. 4, and Fig. 7, wind speed has a significant effect on aerosols after the mature active phase of the SCSSM. However, around day +5, the PBL stratification increasingly stabilizes and the wind speed weakens, which can cause the aerosol extinction coefficient to remain static or perhaps even slightly increase. Determining the exact nature of this change in the extinction coefficient during this stage requires more research into the quantitative relationship between these two factors.

Note that the absorption coefficient has a good relationship between wind speed and PBL stratification in

the active period of the SCSSM. However, under the condition of the unstable PBL stratification and very strong wind speeds during the period of day -2 to +1, the scattering coefficient continues to increase, which contradicts with the analysis above. The specific humidity over the region of 115°-120°E, 22.5°-25°N increases starting at day -1 (Fig. 8b), which corresponds to increased precipitation during the same period (Fig. 8a). This increase in specific humidity and resultant hygroscopic growth could reinforce the aerosol scattering ability (Wu et al.^[26]). Fig. 8c shows a remarkable increase

in aerosol scattering properties during the period from day -1 to +1, which we tentatively attribute to the above aerosol hygroscopic growth. However, the strengthening rainfall and resultant wet deposition clearly reduces the aerosol particles, which causes the aerosol scattering coefficient to decrease after the mature active phase of the SCSSM. Thus, it follows that there is some relationship between the aerosol scattering properties in Guangzhou and the aerosol hygroscopic growth and wet deposition. This aspect of our results also deserves attention and future research.

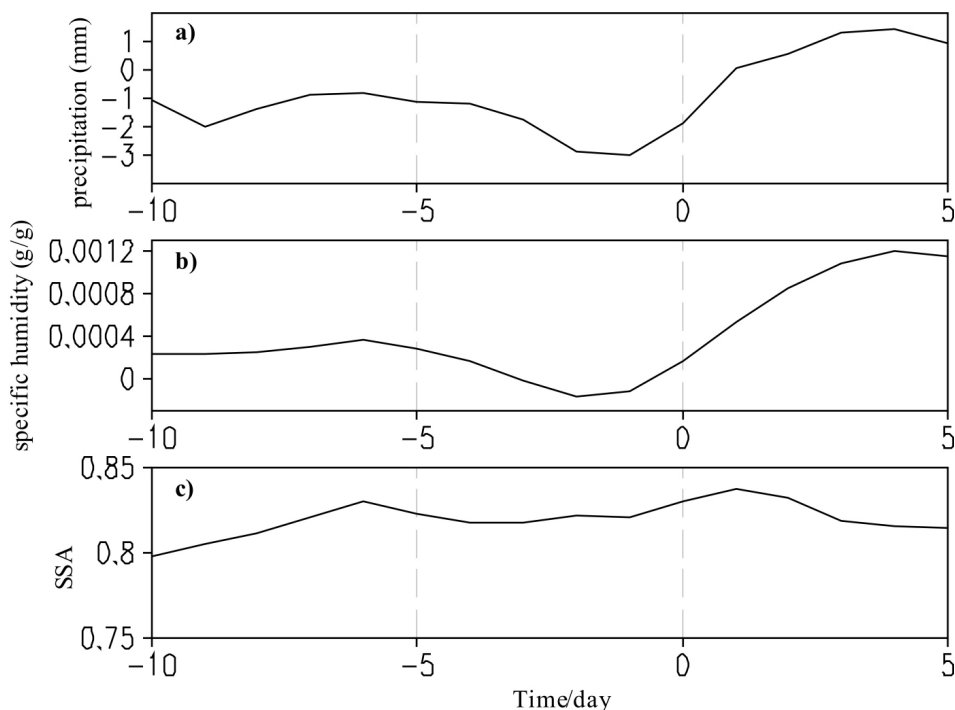


Figure 8. Same as Fig. 3, but for (a) precipitation changes (mm) averaged over 115° to 120°E, 22.5° to 25°N, (b) specific humidity changes (g/g) averaged in the same region, and (c) single scattering albedo in Guangzhou (525 nm).

REFERENCES:

- [1] BABU S S, MOORTHY K K. Anthropogenic impact on aerosol black carbon mass concentration at a tropical coastal station: a case study [J]. *Curr Sci*, 2001, 81 (9): 1 208-1 214.
- [2] MEINRAT, O A. The dark side of aerosols [J]. *Nature*, 2001, 409(6821): 671-672.
- [3] MENON S, HANSEN J, NAZARENKO L, et al. Climate effects of black carbon aerosols in China and India [J]. *Science*, 2002, 297(5590): 2 250-2 253.
- [4] HOUGHTON J T, DING Y, GRIGGS D J, et al. IPCC Climate Change 2001: The Scientific Basis, Radiative forcing of climate change [R], Cambridge, U K, Cambridge University Press, 2001.
- [5] RAMANATHAN V, CRUTZEN P J, MITRA A P, et al. The Indian Ocean experiment and the Asian Brown Cloud [J]. *Curr Sci*, 2002, 83(8): 947-955.
- [6] WON J G, YOON S C, KIM S W, et al. Estimation of direct radiative forcing of Asian dust aerosols with Sun/Sky Radiometer and Lidar measurements at Gosan, Korea [J]. *J. Meteorol Soc Japan*, 2004, 82(1), 115-130.
- [7] LAU K M, RAMANATHAN V, WU G X, et al. The joint aerosol-monsoon experiment: A new challenge for monsoon climate research [J]. *Bull Amer Meteorol Soc*, 2008, 89(3): 369-383.
- [8] JACOBSON M Z. Strong radiative heating due to the mixing state of black carbon in atmospheric aerosols [J]. *Nature*, 2001. 409(6821): 695-697.
- [9] LOHMANN U, LESINS G. Stronger constraints on the anthropogenic indirect aerosol effect [J]. *Science*, 2002, 298 (5595): 1 012-1 015.
- [10] CAO J J, LEE S C, HO K F, et al. Characteristics of carbonaceous aerosol in Pearl River Delta region, China during 2001 winter period [J]. *Atmos Environ*, 2003, 37 (11): 1 451-1 460.
- [11] PENNER J E, DONG X Q, CHEN Y. Observational evidence of a change in radiative forcing due to the indirect aerosol effect [J]. *Nature*, 2004, 427 (6971): 231-234.
- [12] SU Xing-tao, WANG Han-jie and ZHOU Lin. Simulation on spatio-temporal distribution characteristics and radiative forcing of organic carbon aerosols in China [J]. *J Trop Meteor*, 2012, 18(3): 297-304.
- [13] DENG Jie-chun, XU Hai-ming, MA Hong-yun, et al. The

- effects of anthropogenic aerosols over eastern China on East Asian monsoons: Simulation study with a high resolution CAM5.1 model [J]. *J Trop Meteor*, 2014, 30(3): 567-576 (in Chinese).
- [14] REDDY, M S, VENKATARAMAN C. Atmospheric optical and radiative effects of anthropogenic aerosol constituents from India [J]. *Atmos Environ*, 2000, 34(26): 4 511-4 523.
- [15] WANG Yong, JI Zhen-ming, SHEN Xin-yong, et al. Causation analysis of the direct climate effects of anthropogenic aerosols on East-Asian summer monsoon [J]. *J Trop Meteor*, 2013, 29(3): 441-448 (in Chinese).
- [16] CHEN Si-yu, HUANG Jian-ping, QIAN Yun et al. Effects of aerosols on autumn precipitation over mid-eastern China [J]. *J Trop Meteor*, 2014, 20(3): 242-250.
- [17] DEVARA P C S, RAJ P E, PANDITHURAI G, et al. Relationship between lidar-based observations of aerosol content and monsoon precipitation over a tropical station, Pune, India [J]. *Meteorol Appl*, 2003, 10(3): 253-262.
- [18] CHEN W T, LIAO H, SEINFELD J H. Future climate impacts of direct radiative forcing of anthropogenic aerosols, tropospheric ozone, and long-lived greenhouse gases [J]. *J Geophys Res*, 2007, 112, D14209, doi: 10.1029/2006JD008051.
- [19] WANG C, KIM D, EKMAN A M, et al. Impact of anthropogenic aerosols on Indian summer monsoon [J]. *Geophys Res Lett*, 2009, 36, L21704, doi: 10.1029/2009GL040114.
- [20] GU Y, LIU K N, XUE Y, et al. Climatic effects of different aerosol types in China simulated by the UCLA general circulation model [J]. *J Geophys Res*, 2006, 111, D15201, doi:10.1029/2005JD006312.
- [21] HUANG Y, CHAMEIDES W L, DICKINSON R E. Direct and indirect effects of anthropogenic aerosols on regional precipitation over East Asia [J]. *J Geophys Res*, 2007, 112, D03212, doi:10.1029/2006JD007114.
- [22] SOLMON F, MALLETT M, ELGUINDI N, et al. Dust aerosol impact on regional precipitation over western Africa, mechanisms and sensitivity to absorption properties [J]. *Geophys Res Lett*, 2008, 35, L24705, doi: 10.1029/2008GL035900.
- [23] HUANG J, ZHANG C, PROSPERO J M. Large-scale effect of aerosols on precipitation in the West African Monsoon region [J]. *Quart J Roy Meteorol Soc*, 2009, 135(640): 581-594.
- [24] LIN J C, MATSUI T, PIELKE R A, et al. Effects of biomass burning derived aerosols on precipitation and clouds in the Amazon Basin: a satellite based empirical study [J]. *J Geophys Res*, 2006, 111, D19204, doi: 10.1029/2005JD006884.
- [25] WU Dui. A review and outlook on the aerosol study over South China [J]. *J Trop Meteorol*, 2003, 19 (Suppl): 145-151 (in Chinese).
- [26] WU Dui, MAO Jie-tai, DENG Xuejiao, et al. Black carbon aerosols and their radiative properties in the Pearl River Delta region [J]. *Sci China (Ser D)*, 2009, 52(8): 1 152-1 163.
- [27] KALNAY, E, KANAMITSU M, KISTLER R, et al. The NCEP/NCAR 40-year reanalysis project [J]. *Bull Amer Meteorol Soc*, 1996, 77(3): 437-472.
- [28] JANOWIAK, J E, ARKIN P A. Rainfall variations in the tropics during 1986-89, as estimated from observations of cloud-top temperature [J]. *J Geophys Res*, 96 (Suppl.): 3 359-3 373.
- [29] ZHENG Bin, LIN Ai-lan, GU De-jun, et al. Determination of onset date of the South China Sea summer monsoon in 2006 using large-scale circulations[J]. *J Trop Meteorol*, 2011, 17(3): 202-208.
- [30] ZHENG Bin, MENG Wei-guang. The features of South China Sea summer monsoon onset of 2004 and the possible effects of land-surface process in Indo-China Peninsula I: Diagnostic study [J]. *Acta Meteorol Sinica*, 2006, 64 (1): 72-80 (in Chinese).

Citation: ZHENG Bin, WU Dui, LI Fei, et al. Variation of aerosol optical characteristics in Guangzhou during South China Sea summer monsoon events[J]. *J Trop Meteorol*, 2015, 21(1): 76-83.